Experimental description of long time evolution of Akhmediev breathers

O. Kimmoun[1,2], A. Chabchoub[3], H. Branger[2], H.C. Hsu[4], Y.Y. Chen[4], C. Kharif[2], M.S. Li[4].

1 Introduction

Deep water waves in the ocean and wave propagation in optical fibers can be described by the nonlinear Schrödinger (NLS) equation. One class of solutions of this equation is called breather and corresponds to the evolution of solitary waves on finite amplitude background. Due to nonlinear interaction between the solitary waves and the background, the solitons are pulsating. A fundamental analytical solution of these breathers is the Peregrine soliton, which was first presented by Peregrine [1]. The Peregrine soliton is a localized solution in both time and space, and is a limiting case of Akhmediev breathers [2]. For ideal conditions, Peregrine or Akhmediev breathers exhibit only one growth and return cycle. More realistic studies have shown that this behavior is not generally observed and a more complex evolution is observed [3]. In order to verify this complex behavior for water wave, experiments have been conducted in the "mid-size observation Flume" at the Tainan Hydraulics Laboratory (THL) of National ChengKung University, Taiwan. This flume permits to observe the long time evolution of Akhmediev breather.

2 Theoretical preliminaries

The NLS equation describes the evolution in space and time of weakly nonlinear wave trains of amplitude $A(x,t)$ in various media [4]. In finite water depth h it can be derived by applying the method of multiple scales [5, 6] and is given by:

$$-i\left(\frac{\partial A(x,t)}{\partial t}+c_g\frac{\partial A(x,t)}{\partial x}\right)+\alpha\frac{\partial^2 A(x,t)}{\partial x^2}+\beta|A(x,t)|^2A(x,t)=0$$

with

$$\begin{cases}\alpha = & -\frac{1}{2}\frac{\partial^2\omega}{\partial k^2}\\ \beta = & \dfrac{\omega\,k^2}{16\sinh^4(kh)}\left(\cosh(4kh)+8-2\tanh^2(kh)\right)\\ & -\dfrac{\omega}{2\sinh^2(2kh)}\dfrac{(2\omega\cosh^2(kh)+kc_g)^2}{gh-c_g^2}\end{cases}$$

with $\omega^2=gk\tanh(kh)$ and $c_g=\frac{\partial\omega}{\partial k}$. Using rescaling variables:

$$X=x-c_g\,t\quad T=-\alpha\,t\quad\text{and}\quad q(X,T)=\sqrt{\frac{\pm\beta}{2\alpha}}A(X,T)$$

When $kh>1.363$, then $\alpha\beta>0$, and a sign + takes place in the square root. Then the NLS equation becomes:

$$i\,q_T\;+\;q_{XX}\;+\;2\,|q|^2\,q=0$$

In this case, a regular wave train is unstable and the Benjamin-Feir instability grows exponentially. The free surface elevation is given by:

$$\eta(x,t)=\Re\left(A(x,t)\;.\;\mathrm{e}^{i\,(kx-\omega t)}\right)$$

An exact first-order solution of this NLS equation is given by Akhmediev [7]

$$q(X,T)=-\left(1+\frac{2(1-2a)\cosh(2bT)+ib\sinh(2bT)}{\sqrt{2a}\cos(\omega_{mod}X)-\cosh(2bT)}\right)\mathrm{e}^{2iT}$$

[1]email: olivier.kimmoun@centrale-marseille.fr
[2]Aix-Marseille University, CNRS, Centrale Marseille, IRPHE, Marseille, France
[3]Swinburne University of Technology, John St, Hawthorn, Australia
[4]Tainan Hydraulics Laboratory, National Cheng Kung University, Taiwan

with $b = \sqrt{8a(1-2a)}$ and $\omega_{mod} = 2\sqrt{1-2a}$ and with a a parameter related to the period of the wave envelope. An example of $q(X,T)$ for $a = 0.45$ is displayed in Fig.1(Left) and an example of the free surface in front of the wave-maker $\eta(x,t)$ for $x = -70m$ is displayed in Fig.1(Right).

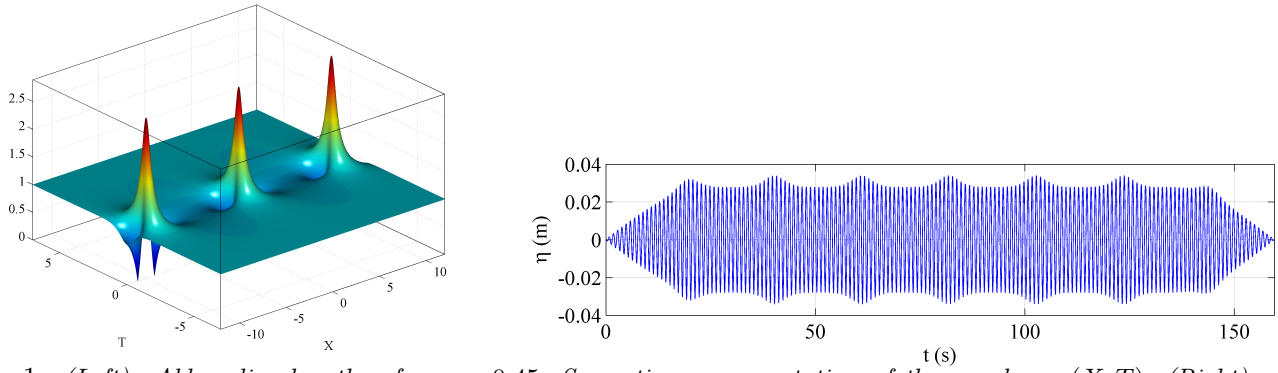

Figure 1: *(Left): Akhmediev breather for $a = 0.45$, Space-time representation of the envelope $q(X,T)$, (Right): wave elevation $\eta(x,t)$ for $x = -70m$ in front of the wave-maker for $T = 1s$, $a_0k = 0.12$ and $a = 0.45$*

3 Experimental setup

Experiments have been conducted at the Tainan Hydraulics Laboratory (THL) of National ChengKung University, Taiwan, in the so-called "mid-size observation flume". This facility is 200m long and 2m wide. The water depth was set to 1.35m. At one end, the tank is equipped with a piston wave-maker and at the other end with an absorbing beach made with rocks. In order to measure wave elevation, 60 capacitance-type wave gauges were used with a sample rate of 100Hz. The first one was located at 2.1m from the wave-maker and the last one at 176.1m. The spatial distribution of the wave gauges is presented in Fig.2.

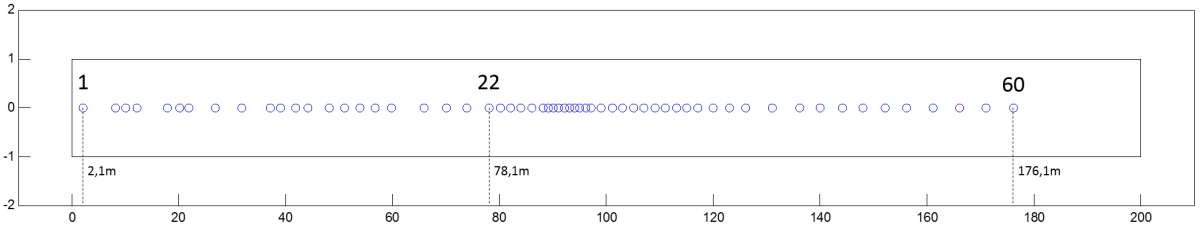

Figure 2: Distribution of the 60 wave gauges along the wavetank

3.1 A weakly nonlinear case

Among all the cases performed during this experiment, a typical case with a small steepness is chosen. In Fig.3(Left), the time evolution of the free surface and the envelope at different wave gauges is displayed. This case corresponds to $T = 1s$, $ak = 0.07$ and $a = 0.45$. In this representation, the x-axis is shifted according to the group velocity in order to have the maxima at the same location. For cases where the steepness is relatively small, the amplitude of the envelope increases and decreases after a maximum is reached, in this case at a distance from the wave-maker equal to 70m. It is noteworthy that the maximum of the envelope is always located at the same place whatever the distance from the wave-maker. In order to estimate the repeatability of the tests, the space evolution of the maximum of the amplitude of the envelope along the tank for three similar wave conditions is displayed in Fig.3(Right). The good agreement between the three curves shows that repeatability is achieved. In the next section, the repeatability for a more nonlinear case (see Fig.5(Left)) is also displayed and shows the same agreement. In Fig.4(Left), the space-time evolution of the envelope is displayed. This figure shows that the evolution of the envelope is regular all along the wave tank. As it can be noticed in Fig.3(Right), for distance to the wave-maker larger than 120m, a second maximum appears just before the main one. This feature is explained in the next section for more nonlinear cases. Another important issue

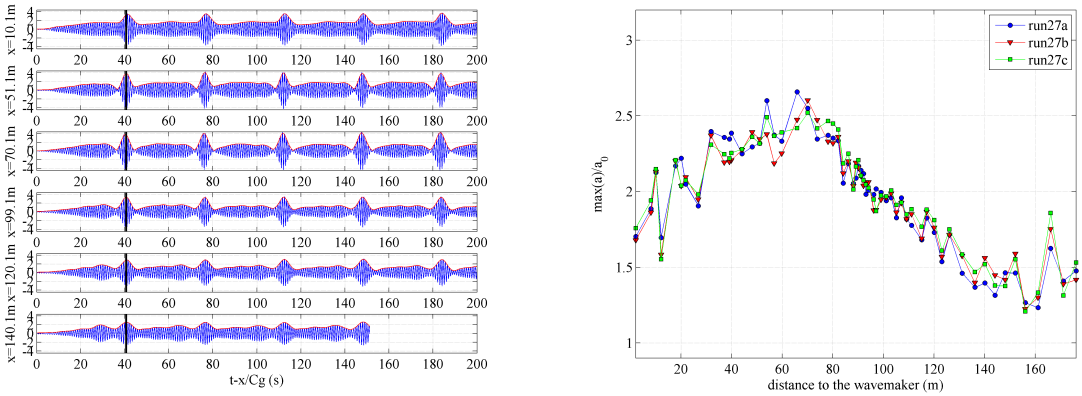

Figure 3: $T = 1s$, $a_0k = 0.07$ *and* $a = 0.45$. *(Left): Time evolution of the free surface and the envelope for different wave gauges. (Right): Space evolution of the maximum of the normalized amplitude of the envelope*

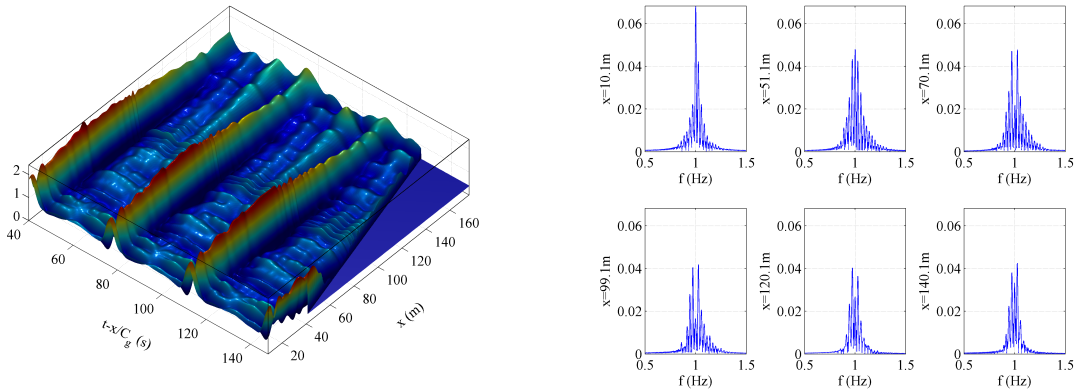

Figure 4: $T = 1s$, $a_0k = 0.07$ *and* $a = 0.45$. *(Left): Time-space evolution of the normalized amplitude of the envelope. (Right): Spectra of the wave elevations for different wave gauges. Values are expressed in* (cm/Hz)

concerns the spectral content of the wave train. In Fig.4(Right), spectra for different wave gauges along the wave tank are displayed. For the wave gauge near the wave-maker, the central peak is dominant with sidebands present on either side of the peak. As the wave train evolves, the central peak decreases up to a minimum and increases again. At the same time, the spectral content of the sidebands increases.

3.2 Highly nonlinear case

While the behavior of the different quantities is relatively simple in the weakly nonlinear case, it becomes more complex when the steepness increases. The considered case corresponds to the same wave period and Akhmediev parameter but for a steepness $ak = 0.12$. In Fig.5(Left) the space evolution of the maximum of the envelope is displayed for three similar tests. Firstly, even for higher values of the steepness, the repeatability is still very good. Secondly, when the steepness increases, we can observed three stages in the evolution: an increasing phase up to a maximum reached at 70m, a decreasing phase up to a minimum reached at 110m and a new increasing phase. In Fig.5(Right) the time evolution of the wave elevation for different wave gauges is presented. As in the previous example, over almost one hundred meters, before the minimum is reached, the maximum is located at the same time. But during the second increasing stage, we can observe that instead of one maximum, two maxima appear at either side of the previous one. This splitting can be observed more easily on the three dimensional representation displayed in Fig.6(Left). This phenomenon has been observed before experimentally for fiber optics by Hammani et al. (2011)[8] and Erkintalo et al. (2011)[9] and corresponds to high-order modulational instability. In these previous experiments, the two subpulses are of the same magnitude. In the present case, the first one with respect to the time is higher than the second one.

As we have presented for the weakly nonlinear case, the spectra for different wave gauges are presented in Fig.6(Right). As in the weakly nonlinear case, the peak at the carrier frequency decreases down to a minimum and increases again. At the same time the frequency contents of the sidebands increase.

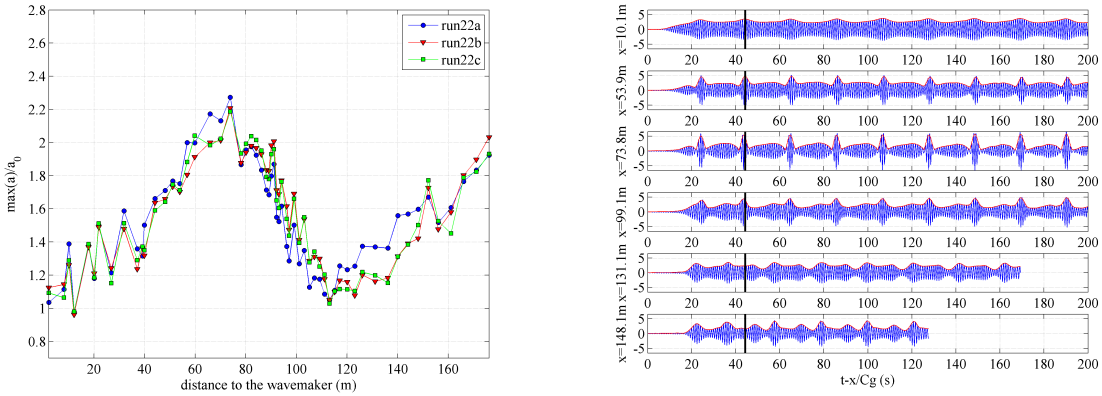

Figure 5: $T = 1s$, $a_0k = 0.12$ *and* $a = 0.45$. *(Left): Space evolution of the maximum of the normalized amplitude of the envelope. (Right): Time evolution of the free surface and the envelope for different wave gauges*

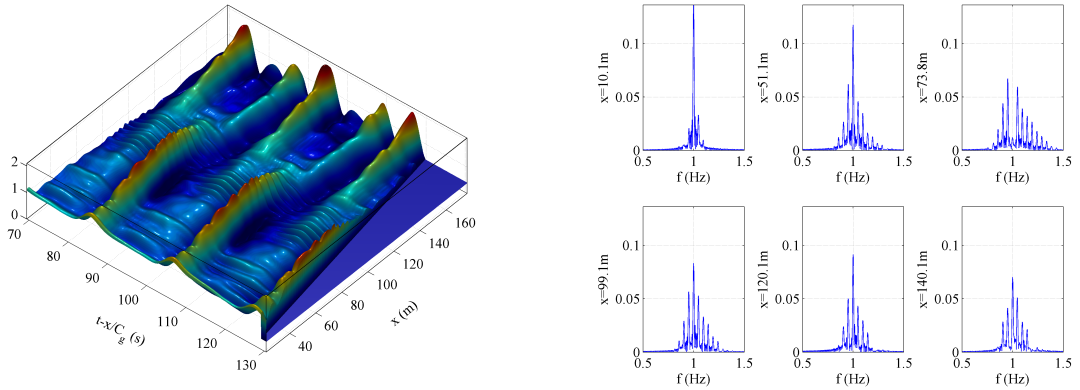

Figure 6: $T = 1s$, $a_0k = 0.12$ *and* $a = 0.45$. *(Left): Time-space evolution of the normalized amplitude of the envelope. (Right): Spectra of the wave elevations for different wave gauges. Values are expressed in* (cm/Hz).

References

[1] D. H. Peregrine (1983). Water waves, nonlinear Schrödinger equations and their solutions. The Journal of the Australian Mathematical Society. Series B. Applied Mathematics, 25, pp 16-43.

[2] N. Akhmediev and V. I. Korneev, (1986) Modulation instability and periodic solutions of the nonlinear Schödinger equation, Theor. Math. Phys. (USSR) , 69, 1089-1093.

[3] Akhmediev N. N. and Ankiewicz A., (1997), Solitons, Nonlinear Pulses and beams, Chapman and Hall, London.

[4] V. E. Zakharov, (1968), Stability of periodic waves of finite amplitude on a surface of deep fluid, J. Appl. Mech. Tech. Phys. 2, 190–194.

[5] H. Hasimoto, and H. Ono, (1972), Nonlinear modulation of gravity waves, J. Phys. Soc. Japan 33, 805–811.

[6] C. C. Mei, (1983), ,The Applied Dynamics Of Ocean Surface Waves, Advanced Series on Ocean Engineering 1.

[7] N. N. Akhmediev, V. M. Eleonskii and N. E. Kulagin, (1987), Exact first-order solutions of the nonlinear Schrödinger equation. Theoretical and mathematical physics, 72(2), 809–818.

[8] K. Hammani, B. Kibler, C. Finot, P. Morin, J. Fatome, J. Dudley and G. Millot, (2011), Peregrine soliton generation and breakup in standard telecommunications. Optics Letters, Optical Society of America, 36 (2), pp.112-114.

[9] M. Erkintalo, K. Hammani, B. Kibler, C. Finot, N. Akhmediev, J.M. Dudley and G. Genty, (2011), Higher-order modulation instability in nonlinear fiber optics, Physical Review Letters 107, 253901.